



Article

# Natural Cellulose from *Ziziphus jujuba* Fibers: Extraction and Characterization

Aicha Amior <sup>1</sup>, Hamid Satha <sup>1,\*</sup>, Fouad Laoutid <sup>2,\*</sup> , Antoniya Toncheva <sup>2</sup> and Philippe Dubois <sup>2</sup> <sup>1</sup> Laboratoire LSPN, Université 8 Mai 1945 Guelma, BP 401, Guelma 24000, Algeria<sup>2</sup> Laboratory of Polymeric and Composite Materials, Materia Nova Materials R&D Center & UMons Innovation Center, 7000 Mons, Belgium

\* Correspondence: satha.hamid@univ-guelma.dz (H.S.); fouad.laoutid@materianova.be (F.L.)

**Abstract:** Nowadays, due to their natural availability, renewability, biodegradability, nontoxicity, light weight and relatively low cost, natural fibers, especially lignocellulosic fibers, present attractive potential to substitute non-eco-friendly synthetic fibers. In this study, *Ziziphus jujuba* fibers were used, thanks to their low lignin content, as an alternative of renewable resource for the production of cellulosic fibers with suitable characteristics and minimal time and energy consumption. In fact, due to their valuable chemical composition, it was possible to remove the amorphous fractions and impurities from the fiber surface by applying ultrasounds coupled with alkaline treatment (80 °C, 5 wt.% NaOH), followed by a bleaching step. The efficient dissolution of the noncellulosic compounds was confirmed by Fourier Transform Infrared Spectroscopy (FTIR). The resulted increase in the crystallinity index (from 35.7% to 57.5%), occurred without impacting the crystalline structure of the fibers. The morphological analysis of the fibers evidences the higher surface area of the obtained fibers. Based on the obtained results, *Ziziphus jujuba* fibers were found to present a suitable sustainable source for the production of cellulosic fibers.

**Keywords:** *Ziziphus jujuba* fibers; cellulose fibers; physicochemical properties; alkaline treatment; thermal stability



**Citation:** Amior, A.; Satha, H.; Laoutid, F.; Toncheva, A.; Dubois, P. Natural Cellulose from *Ziziphus jujuba* Fibers: Extraction and Characterization. *Materials* **2023**, *16*, 385. <https://doi.org/10.3390/ma16010385>

Academic Editors: Pavel Kopel and Ewelina Jamróz

Received: 1 December 2022

Revised: 20 December 2022

Accepted: 27 December 2022

Published: 31 December 2022



**Copyright:** © 2022 by the authors. Licensee MDPI, Basel, Switzerland. This article is an open access article distributed under the terms and conditions of the Creative Commons Attribution (CC BY) license (<https://creativecommons.org/licenses/by/4.0/>).

## 1. Introduction

The growing environmental concerns and the expected depletion of fossil resources require the design and development of new energy-efficient and environmentally friendly processes and materials. In this spirit, harnessing the abundance and the unique diversity of biomass, effective, renewable and biodegradable raw materials, such as lignocellulosic fibers, present a great interest [1,2]. In addition, these fibers are flexible in processing, lightweight and low-cost compared to conventional synthetic fibers (e.g., carbon, glass, nylon and aramids). As a result of these desirable properties, cellulosic fiber is becoming increasingly popular as a functional biomaterial [3].

Cellulose is the most abundant natural polymer on our planet. Each year, nature produces more than 10<sup>10</sup> tons of cellulose, representing more than half of the biomass on Earth. In term of chemical structure, cellulose is a linear homopolymer of glucose residues of configuration D, connected in a β-(1–4) glycosidic bond that can be extracted from many sources, such as algae and higher plants; among them, seeds, stalks, leaves, barks, fruits and roots are the most plant parts used [4,5]. Various chemical treatments aiming to isolate the cellulose fibers from raw plants, such as alkali treatment and bleaching, have been explored. These treatments are used to remove the amorphous fractions and impurities from the fiber surface, enhancing its chemical composition and subsequently the final material mechanical properties, surface morphology, crystallinity index and thermal stability [6]. However, due to the considerable time consumption, energy and expense by such treatments, these processes are often combined with some green chemistry extractions based on ultrasound and microwave irradiation approaches [7]. Consequently, the mechanical, optical, thermal

and physical properties of the extracted cellulose-based materials are largely determined by the plant source and extraction method [8].

The exceptional physical and chemical properties of cellulose fibers are making them valuable fillers in the concept and development of polymer (nano)composites characterized by high thermomechanical properties [9]. Nonwoven mat fibers, short fibers, woven fibers, microfibrils, nanofibrils and nanocrystals are examples of plant-based fibers known to improve the mechanical properties of polymers. In addition to their excellent mechanical properties (Young's modulus as high as 138 GPa), cellulosic fibers possess a high aspect ratio and a high active surface, favoring their surface modification for fine-tuned surface chemistry. As a result, their application can be extended to medicine, pharmaceuticals, automotives, construction, food packaging and water purification [10,11]. Considering the present environmental and ecological context, it is of common interest to develop new approaches that are oriented towards exploiting natural resources, thus addressing and managing the growing industrial needs, which are not yet aligned with the current cellulosic fiber production.

Interestingly, several reports have dealt with natural cellulosic fiber separation from various natural sources such as artichoke, bamboo, banana, coir, cotton, flax, grass, hemp, jute, okra, pineapple, ramie, sisal and wheat [12]. Even though *Ziziphus jujuba* plants are abundant in different geographic regions, e.g., in China, Iran, Africa, South Korea, Cyprus, Spain, Greece and Sicily, little is known about their natural cellulosic fiber. The *Ziziphus jujuba* plant, also known as jujube, belongs to the Rhamnaceae family, including up to 170 species of *Ziziphus*. In Arab countries, the jujube tree is commonly called sidr, nabk and anneb, while in China it is called Chinese date. Over the recent years, especially in traditional medicine, several parts of *Ziziphus jujuba* have been used in clinical practice as antiurinary agents, antidiabetics, antidiarrhea agents, insomnia agents and sedatives, as well as for infections, bronchitis and hypoglycemic activities [13,14].

The purpose of this study is to evaluate the potential of *Ziziphus jujuba* fiber to replace commonly used non-eco-friendly synthetic fibers across various fields of application. For this purpose and for the first time, the extraction and characterization of a novel variety of cellulose from bleached and delignified *Ziziphus jujuba* fiber as a natural source and as a filler for the development of biodegradable composite materials is proposed. As part of the study, multiple analytical methods (FTIR, TGA, XRD, UV-vis and SEM) were used to investigate the impact of mechanical and chemical treatments on fiber morphology, structure, and thermal characteristics. The obtained fiber properties were also compared to those of other lignocellulosic fibers.

## 2. Materials and Methods

### 2.1. Materials

*Ziziphus jujuba* stems (Figure 1a) were kindly provided by the Faculty of Pharmacy, University Badji Mokhtar Annaba, Algeria. Before their use, they were cut into small pieces, then washed with distilled water to reduce impurities and dried at room temperature. A domestic coffee grinder (Moulinex AR 110830) was used to grind the dry matter to a fine powder (Figure 1b).

Various chemicals with a high degree of purity (>99%), supplied by Aldrich, were used in this work without any further purification: sodium hydroxide, hydrochloric acid, chloroform, methanol, acetone, sodium chlorite and glacial acetic acid. An ultrasound water bath was used for the present experiments.



**Figure 1.** Photographs of (a) *Ziziphus jujuba* plant, (b) untreated *Ziziphus jujuba* material, (c) alkali-treated samples and (d) final bleached cellulose.

## 2.2. Isolation of Cellulose

Cellulose was isolated in several steps using the procedure described elsewhere [15–18], with some specific modifications. Briefly, 20 g of *Ziziphus jujuba* stem powder was preliminarily dispersed in a chloroform/methanol (2:1 *v/v*) mixture for 2 h to remove all substances soluble in organic solvents (pigments, lipids and waxes) and washed with hot water for 1 h. Next, the obtained powder was submitted to an alkali treatment at 80 °C with NaOH solution (5%) for removing hemicelluloses and lignins. After 8 h, the fibers were rinsed several times with distilled water until reaching neutral pH. To ensure complete delignification, the alkali-pretreated sample was bleached using a solution of sodium chlorite (1.7 wt.% NaClO<sub>2</sub> in water) and sodium acetate buffer at pH = 4.8 in the ratio 1:1 (*v/v*) at 80 °C for 3 h. The operation was repeated until the cellulose fibers turned white and finally lyophilized (−85 °C, 0.0014 mbar, 12 h). All the previously described treatments were performed in an ultrasonic water bath (Elma 100, 40 kHz).

## 2.3. Characterization Methods

### 2.3.1. Chemical Analysis

The standard NREL technique (NREL/TP-510-42,618), described previously by Sluiter [19], was used for determining the weight content of cellulose, hemicellulose and lignin in the fibers, before and after alkali treatment through high-performance liquid chromatography (HPLC) analysis. Water:acetonitrile was used as mobile phase at 40 °C. The gas pressure was fixed at 3 bar. In brief, the fibers were hydrolyzed with sulfuric acid and the insoluble fraction was used for determining lignin content, while the glucose, xylose and arabinose contents were determined on the soluble fraction. In relation to the initial solid fraction, the weight content of glucose corresponded to the content of cellulose, while the sum of the xylose and arabinose contents was related to the hemicellulose content.

### 2.3.2. Fourier Transform Infrared (FTIR) Spectroscopy

FTIR spectra were recorded using a Thermo Scientific Nicolet iS50 spectrometer based on smart iTX-Diamond fitted with an ATR (attenuated total reflectance) system in the range of 500–4000  $\text{cm}^{-1}$  with a resolution of 4  $\text{cm}^{-1}$  and an accumulation of 32 scans. The samples were placed directly into their compartments, without any prior treatment. The analysis was performed at room temperature.

### 2.3.3. X-ray Diffraction Analysis (XRD)

XRD analysis was performed under ambient conditions using a Bruker D8 ECO diffractometer with a voltage of 40 kV and an intensity of 25 mA in the range of  $5^\circ < 2\theta < 80^\circ$ . The crystallinity index (CI) was obtained according to the empirical Segal method [20], by calculating the ratio of the crystallized area to the total area, as shown in Equation (1):

$$\text{CI \%} = \left[ \frac{I_{200} - I_{\text{AM}}}{I_{200}} \right] \times 100 \quad (1)$$

where  $I_{002}$  is the maximum intensity of crystalline region and  $I_{\text{am}}$  is the lowest intensity of amorphous region.

The Scherrer Equation (2) was used to calculate crystallite size (CS) [21]:

$$\text{CS} = \frac{k\lambda}{\beta \cos \theta} \quad (2)$$

where  $k$  is the Scherrer constant (0.9),  $\lambda$  is the X-ray wavelength (0.154 nm),  $\theta$  is the Bragg angle and  $\beta$  is the peak full width at half maximum (FWHM).

### 2.3.4. Scanning Electron Microscopy (SEM)

The evolution of fiber morphology (fibrillation and surface morphology) was performed by scanning electron microscopy. The surface morphology of the samples was recorded using a JEOL 840 A LGS with a voltage of 5 kV.

### 2.3.5. Thermogravimetric Analysis (TGA)

Thermal decompositions of the different fibers were studied by thermogravimetric analysis (TGA) under nitrogen. Approximately 10 mg of the sample was submitted to a temperature ramp from 40 to 800  $^\circ\text{C}$  at a heating rate of 10  $^\circ\text{C}/\text{min}$  using Netzsch STA449 F3 Jupiter, Germany.

## 3. Results

### 3.1. Chemical Composition

Cellulose, hemicellulose and lignin represent the majority of the lignocellulosic biomass, and their amounts are greatly dependent on the climatic conditions, age of the plant, soil condition and extraction methods, which thus induce a difference in the fibers' technical performances, such as thermal, mechanical and biodegradable properties [22].

The chemical composition of untreated and alkali treated *Ziziphus jujuba* fibers is compared with various natural fibers in Table 1. The amounts of cellulose, hemicellulose and lignin of the raw fibers were determined to be around 43.0 wt.%, 10.2 wt.% and 5.1 wt.%, respectively. By means of hydrogen bonds and other linkages, cellulose provides high tensile properties to *Ziziphus jujuba* fibers, while hemicellulose and lignin help to maintain the strength of the fiber and to hold water inside for protection against bioattacks.

Alkali treatment changes the chemical composition of fibers significantly. Indeed, the cellulose fraction of *Ziziphus jujuba* fibers increased from 43% to 52% while hemicellulose and lignin fractions were reduced by 4.5% and 2.9%, respectively. This change is due to the breakdown of the ester bonds and  $\alpha$ -ether linkages between hydroxyl groups of lignin and carboxylic groups of hemicellulose, which promotes the dissolution of hemicellulose and lignin [23]. Increasing the cellulose content is a desirable effect as cellulose improves the



mechanical properties of fibers. In addition, more hemicellulose and lignin can be removed by extending treatment times [24]. However, increasing the concentration of the chemical agents and treatment duration results in lower yields of cellulose fibers due to the breaking of glycosidic bonds, and thus the depolymerization of polysaccharides [25].

Fibers from leaves (abaca) or bast plants (jute, hemp and ramie), which are frequently used in the manufacture of composite materials [26–28], generally have the highest cellulose content. These robust fibers clearly possess superior mechanical properties with regards to other plant fibers.

**Table 1.** Comparison of chemical composition of *Ziziphus jujuba* fiber before and after alkali treatment with other natural fibers.

Fiber Name	Cellulose (wt.%)	Hemicellulose (wt.%)	Lignin (wt.%)	Reference
<i>Zizyphus jujube</i>	43.0	10.2	5.1	Present study
5% alkali-treated <i>Zizyphus jujube</i>	52.0	5.7	2.2	
<i>Leucas Aspera</i>	50.7	13.2	9.7	[29]
<i>Catharanthus roseus</i>	47.3	9.1	15.1	[30]
<i>Eleusine indica</i> grass	61.3	14.7	11.1	[31]
Abaca	56.0–63.0	15–17	7–10	[26]
Jute	72.0	13.0	13.0	[27]
Hemp	74.0	18.0	4.0	[27]
Ramie	68.6–72.6	13.1–16.7	0.6–0.7	[26]
Saharan aloe vera	67.4	8.2	13.7	[32]
Cotton	85–90	1–3	0.7–1.6	[33]
Sisal	78.0	19.0	8.0	[34]
Bamboo	26–43	30	21–31	[35]
Shwetark	69.6	0.2	16.8	[36]
Flax	81.0	14.0	3.0	[27]
Aerial roots of banyan tree	67.3	13.5	15.6	[37]
Manau rattan ( <i>Calamus manan</i> )	42.0	20.0	27.0	[3]
<i>Dracaena reflexa</i>	70.3	11.0	11.4	[38]
<i>Ficus religiosa</i> tree	55.6	13.9	10.1	[39]
Napier grass	45.7	33.7	20.6	[40]
Bagasse	55.2	16.8	25.3	[41]
Cabuya	68–77	4–8	13.0	[42]
<i>Manicaria saccifera</i> palm	74.1	12.0	31.1	[43]
<i>Linum usitatissimum</i>	85.0	9.0	4.0	[44]

### 3.2. Physical Appearance

The evolution of the macroscopic aspect of the fibers at each stage of cellulose isolation is presented in Figure 1. As can be seen, there is a change in the color of the materials obtained after each treatment. These results indicate that the compounds targeted by the applied process have been removed. The effectiveness of the alkaline treatment was indicated by the light brown color, revealing that majority of the hemicelluloses were taken off (Figure 1c). After the bleaching treatment (Figure 1d), the light brown color evolved into a white color, a clear indication of near-pure cellulosic material. In this meaning, it can be concluded that the noncellulose constituents such as lignin, hemicellulose, pectin and wax were effectively removed during the bleaching treatment.

### 3.3. FTIR Analysis

Analysis by infrared spectroscopy was used to explore the alterations in the functional groups caused by different treatments undergone by *Ziziphus jujuba* fibers. The FTIR spectra of the untreated, the alkali-treated and the cellulose fibers are presented in Figure 2 and the main characteristic bands are summarized in Table 2.

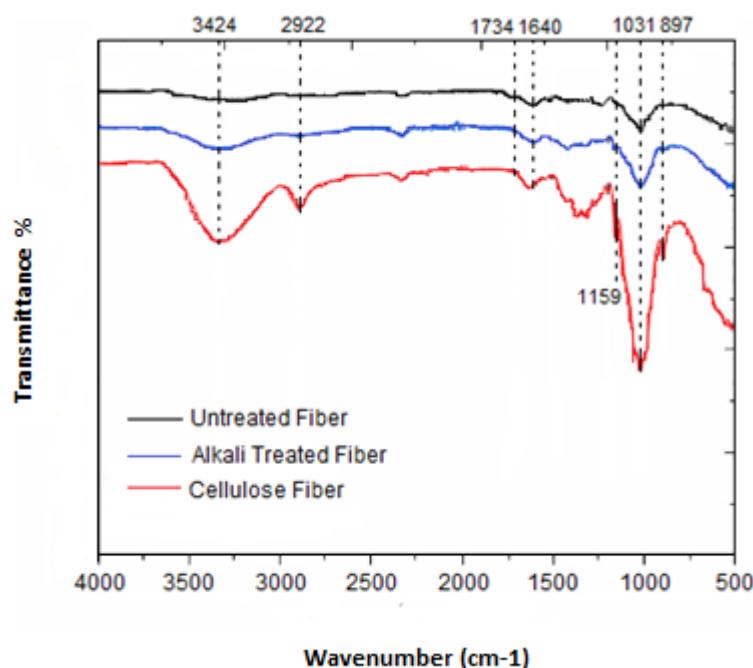


Figure 2. FTIR spectra of untreated, alkali-treated and cellulose fibers.

Table 2. Characteristic bonds of different compounds of *Ziziphus jujuba* fiber.

Characteristic Bands (cm <sup>-1</sup> )		Cellulose	Lignin	Hemicellulose
3424	-OH	✓	✓	-
2922	C-H	✓	✓	✓
1734	C=O	-	✓	✓
1508	C=C	-	✓	-
1429	CH <sub>2</sub> , CH <sub>3</sub>	✓	✓	✓
1054	C-O, C-O-C	✓	-	-

For all the samples, characteristic O-H stretching vibration bands (3424 cm<sup>-1</sup>) of the inter and intramolecular hydrogen bonds revealing the hydrophilic trend of the fibers were present. In the cellulose fiber, this characteristic band was more intense, indicating higher cellulose content due to the elimination of lignin and hemicellulose [45]. The characteristic band at 2922 cm<sup>-1</sup> was attributed to the stretching vibration of the sp<sup>3</sup> C-H group, and the H-O-H stretching vibration as result of the absorbed water appeared at 1640 cm<sup>-1</sup>. A more pronounced intensity was found in the case of cellulose as compared to both untreated and alkali-treated fibers due to the higher moisture content in this sample [46]. Furthermore, the extraction of the amorphous phase (lignin and hemicellulose) after chemical treatments was confirmed by the disappearance of the compound characteristic absorption bands: (i) the first one at 1734 cm<sup>-1</sup> corresponds to the C=O stretching vibration of p-coumaric acids of lignin and/or hemicellulose; (ii) a second band related to either acetyl or ester linkages of carboxylic groups of the ferulic or uronic ester groups in hemicellulose [47]; (iii) the other absorption bands at 1508 cm<sup>-1</sup> and 1236 cm<sup>-1</sup> correspond to the C=C bond strain of the aromatic ring of lignin and the C-O stretching of the aryl group C=O-O vibration of acetyl groups, respectively. The disappearance of these bands is due to the breakage of carboxylic ester bonds and the oxidation of terminal glucopyranose units [47]. The two bands at 1429 cm<sup>-1</sup> and 1327 cm<sup>-1</sup> are attributed to the vibrations of C-C bonds in the CH<sub>2</sub>, CH<sub>3</sub> groups and to the C-O skeletal vibrations, respectively, while the band at 1054 cm<sup>-1</sup> is assigned to the ether C-O binding vibrations [48]. The C-O-C pyranose ring skeletal vibration appears at 1031 cm<sup>-1</sup>. The increase in the percentage of cellulosic components after the successive pretreatments is evidenced by the presence of the typical

peaks ascribed to cellulose at  $1159\text{ cm}^{-1}$  and  $897\text{ cm}^{-1}$ , corresponding to the asymmetric stretching vibration of the C-O-C and the  $\beta$ -(1 $\rightarrow$ 4)-glycosidic bonds of glucose rings [49,50].

### 3.4. Crystallinity Analysis

Based on previously published data, it is known that the quantity of cellulose component of fibers affects their crystallinity [51]. Accordingly, it was of importance to study this parameter in detail, and X-ray diffraction analysis was performed. The X-ray diffractograms of untreated, alkali-treated and cellulose fibers are shown in Figure 3. The degree of crystallinity varies considerably with the fiber origin and with the physical and chemical treatments to which it has been subjected [51].

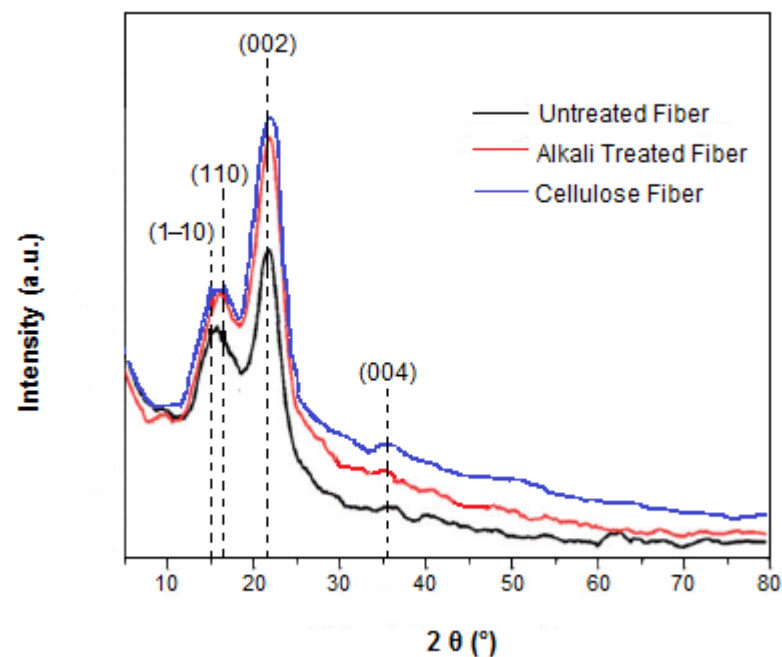


**Figure 3.** X-ray diffractograms of untreated, alkali-treated and cellulose fibers.

The general profile of the three diffractograms is similar. The  $2\theta$  values ranging between  $10^\circ$  and  $40^\circ$  display same main peaks at  $15.0^\circ$ ,  $16.20^\circ$ ,  $21.85^\circ$  and  $35.4^\circ$ . These  $2\theta$  values were ascribed to the following crystallographic planes: (1-10), (110), (002) and (004), corresponding to the typical structure of cellulose I, conferring the material rigid nature. The existence of other fractions such as lignin, hemicellulose, amorphous cellulose and pectin in the fibers was confirmed by the presence of diffraction peaks at  $2\theta$  values of  $16.2^\circ$ , while the content of  $\alpha$ -cellulose was assigned by the peak at  $2\theta$  values of  $21.85^\circ$  [52]. In general, the direction and alignment of the fibers are signed by the peak  $2\theta$  located at  $35.4^\circ$  [53]. Since they contain diffraction peaks characteristic for the amorphous phase ( $16.2^\circ$ ), as well as diffraction peaks unique for the crystalline phase ( $15^\circ$ ,  $21.85^\circ$  and  $35.4^\circ$ ), it can be concluded that the obtained diffractograms are typical of semicrystalline material. The diffraction peaks at  $15^\circ$  and  $16.2^\circ$  were assigned to the principal equatorial planes indexed at (1-10) and (110) in the monoclinic cell with two chains. For a high percentage of cellulose I (high crystallinity degree), these two diffraction peaks were present and distinct from each other. Conversely, when the fibers contain a high percentage of amorphous phase (lignin, pectin and hemicellulose fraction), a single common diffraction peak is observed.

The structural transformation from cellulose I to cellulose II was not observed in the present study due to the low alkaline concentration used (5 wt.%). This result agreed with the finding described by Yue et al. [54], where the conversion from cellulose I to cellulose II could not be reached when treating cellulose-based fibers with less than 10 wt.% of NaOH. Based on the obtained findings, it can be concluded that the structure of cellulose I

was largely preserved in all the samples. The crystallinity indices are determined for the various samples and reported in Table 3. Crystallinity index is a factor used to exemplify the relative quantity and the order of the crystallites in the fibers [51].

**Table 3.** Crystallinity index and crystallite sizes of untreated, alkali-treated and cellulose fibers.

Samples	Crystallinity Index (%)	Crystallite Size (nm)
Untreated fiber	35.70	16.30
Alkali-treated fiber	50.81	12.81
Cellulose fiber	57.51	10.12

According to Table 3, the untreated, alkali-treated and cellulose fibers exhibit a crystalline index of 35.70%, 50.81% and 57.51%, respectively. As a result of the successive elimination of low-molecular-weight compounds (amorphous lignin, hemicellulose and impurities—waxes and pectin) by the applied alkali and bleaching treatments, the amount of crystalline cellulose fraction proved to be enhanced. As a result, the crystals became more regularly arranged and favored an increase in the CI values, as shown by the higher (200) reflection intensity in chemically treated fibers with respect to the raw fibers.

This finding was in good agreement with the results reported by Zhao et al. [23] and Ciftci et al. [55], for cellulose fibers from poplar wood and canola straw, respectively. It is expected that the strength and stiffness of the fibers are influenced by the treatment steps and they are increased by the improved crystallinity [56].

Crystal size is also known to affect water absorption capacity of the fiber [51]. The average size of a sole crystal was found to be 16.3 nm, 12.81 nm and 10.12 nm for untreated, alkali-treated and cellulose fibers, respectively. The larger CS of raw fiber may be due to the presence of aggregate precipitation and some larger filaments, which affect the chemical reactivity and the mechanical strength of the fibers. A reduction in the crystallite sizes after the surface treatment was observed. In addition, the decrease in the crystallite sizes affected the constricted packing of crystallites and considerably decreased the moisture permeation, which reduced the hydrophilic behavior of the fiber. The crystallite sizes of the fiber may be increased or decreased depending on the source of the fiber and the extraction process, as reported by Cullity [57]. The high crystallinity index and low crystal size of the cellulosic fiber were found to be favorable factors for producing durable biocomposites [58].

### 3.5. Thermal Properties

The thermal stability of natural fibers is an important property that determines their suitability for different industrial applications and compatibility with polymer melt processing conditions. In order to evaluate whether the chemical treatment induced changes in the thermal stability of the fibers, a TGA was performed on the untreated, alkali-treated and cellulose fibers, as shown in Figure 4. The onset ( $T_{\text{onset}}$ ) and the maximum ( $T_{\text{max}}$ ) degradation temperatures of the samples are listed in Table 4.

**Table 4.** Thermal degradation temperatures and charred residue of *Ziziphus jujuba* fibers before and after different treatments (10 °C/min, under N<sub>2</sub>).

Samples	$T_{\text{onset}}$ (°C)	$T_{\text{max}}$ (°C)	Charred Residue (%)
Untreated fiber	175	335	19.1
Alkali-treated fiber	215	360	8.1
Cellulose fiber	220	362	5.2



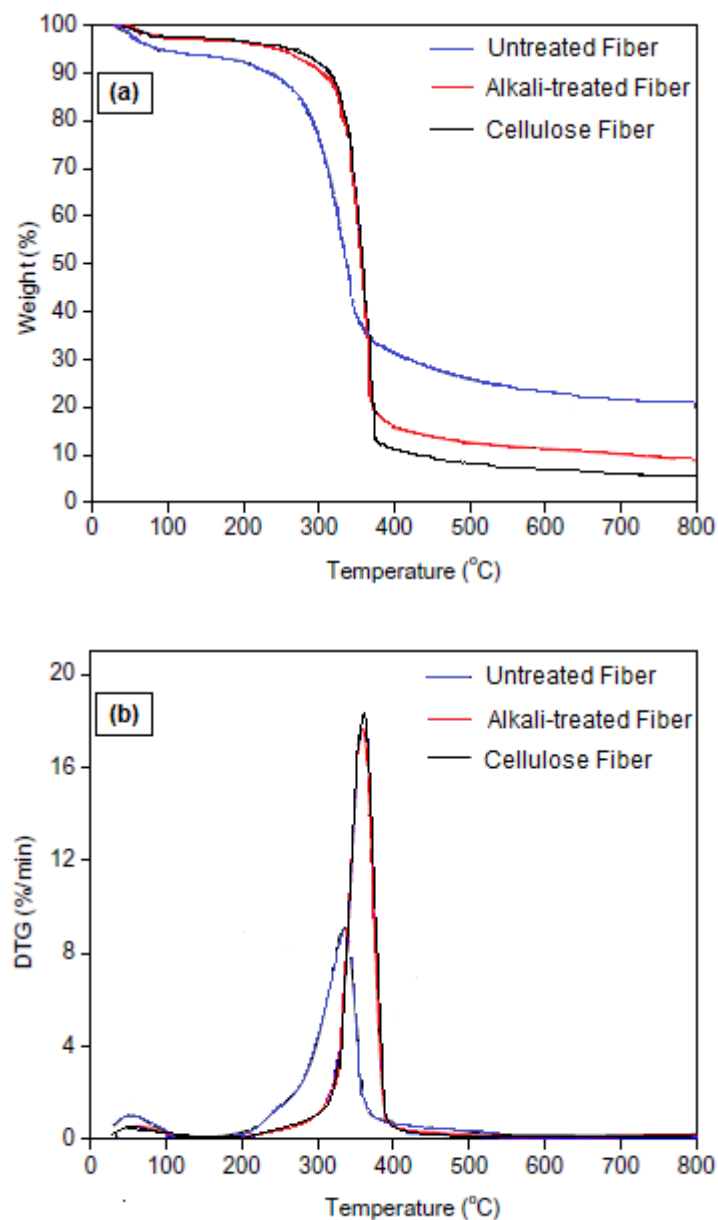


**Figure 4.** (a) TG and (b) DTG thermograms of the untreated, alkali-treated and cellulose fibers.

The difference in the thermal stability of lignocellulosic fibers can be attributed to some variation of the fiber chemical structure and related physical properties [58]. One can observe that the three fibers present some difference in weight loss below 100 °C, i.e., 6.8 wt.%, 3.9 wt.% and 3.1 wt.% for untreated, alkali-treated and cellulose fibers, respectively. This weight loss corresponds to the release of both moisture and bound water [59]. The thermal degradation of the other constituents occurs at different temperature ranges. Cellulose is more thermally resistant than hemicellulose because of the decarboxylation of the glycosidic linkages [60]; its degradation occurs between 300 °C and 420 °C, while hemicellulose degrades between 190 °C and 300 °C [60]. Lignin thermal degradation is a complex process that takes place over a wide temperature range between 200 °C and 600 °C, occurring in different steps due to its intricate structure with numerous branches of oxygen-based functional groups such as phenolics and aromatics [61]. Untreated fibers present thermal stability lower than the other two fibers due to the presence of hemicellulose in the fibers before treatment.

Chemically-treated fibers have one degradation stage, while untreated fibers visibly display two stages associated to the degradation of numerous components such as cellulose,

hemicellulose and lignin, which are usually renowned for their dissimilar degradation temperatures. The first stage appears in the DTG thermograms as a shoulder between 175 °C and 275 °C and the second one appears as a prominent peak between 275 °C and 375 °C. Therefore, the chemically treated fibers revealed higher onset decomposition at 215 °C and 220 °C for the alkali-treated and cellulose fibers, respectively, when compared to the raw fibers at 175 °C. This increase in the onset thermal degradation temperature is ascribed to the elimination of amorphous hemicellulose and lignin, known for their low decomposition temperatures. It is worth noting that the onset degradation temperature of cellulose fibers is influenced by the crystallinity index, degree of polymerization and hydrogen bond energy [62]. The thermal stability of the untreated *Ziziphus jujuba* fiber is relatively lower than the chemically treated fibers.

### 3.6. Morphological Analysis

As a next step, it was important to examine the surface morphology of *Ziziphus jujuba* fiber before and after different treatments. This approach will allow one to understand the distribution of various constituents present over the fiber surface. The SEM analysis was performed in the longitudinal direction at different magnifications, as shown in Figure 5.

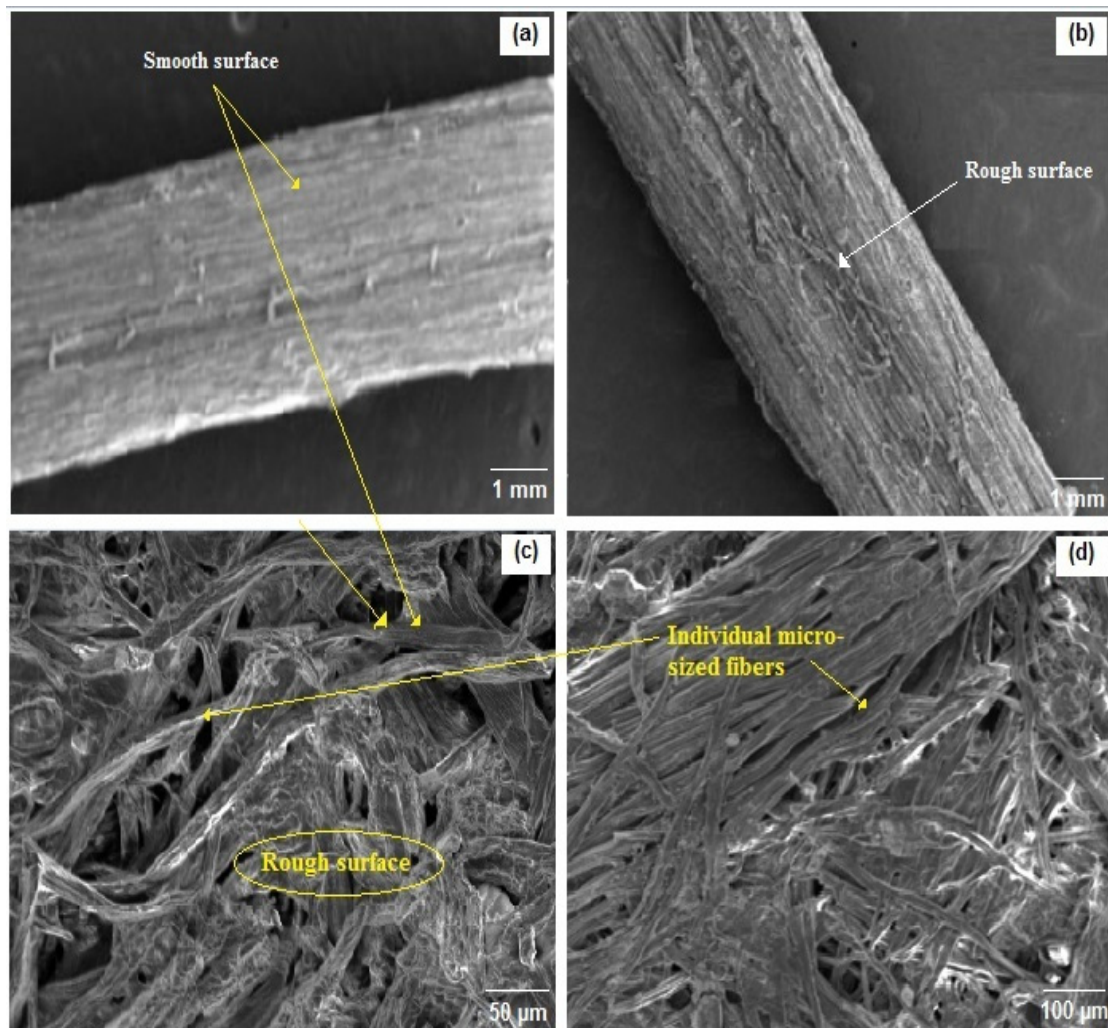


**Figure 5.** SEM micrographs of (a) untreated, (b) alkali-treated and (c,d) cellulose fibers.

As evidenced from SEM micrographs, the alkali and bleach treatments of the fibers induced some morphological changes as a result of the dissimilarity in the operational conditions.

Before any treatment, the cellulose chains are oriented and joined together by cement components (lignin and hemicellulose), forming thickly packed fiber bundles of a certain diameter with a complex structure. Significant magnification of 1 mm (Figure 5a,b) shows that the *Ziziphus jujuba* fiber is quite cylindrical, which grows the specific area and thus is nepotistic to the chemical processes. In addition, the raw fiber (Figure 5a) showed a partially smooth surface due to the deposition of a waxy layer on its outside [63]. Some discrete white-colored and undersized patches adhered on the surface of the fibers, which may be impurities or noncellulosic elements. The mechanical properties, and thus the interfacial union for biocomposites, are conditioned by the presence of these impurities. With partial elimination of some quantities of outer-layer components such as hemicellulose, lignin, wax and other impurities, many irregularities are present on the surface of the alkali-treated fibers, increasing their roughness texture compared to the raw fibers (Figure 5b). The increase in roughness is favorable for composite materials due to the enhanced adherence to the fiber with the matrix. An enhancement of flax/epoxy polymer interfacial adhesion by alkali treatment was reported by Yan et al. [64]. After NaOH treatment, a slight variation in the diameter of fiber bundles was observed as result of partial removal of lignin. Lignin is a component displaying binding ability in fibers and constituting a bridge link with cellulose, thus preserving its bundle-like morphology after NaOH treatment [65]. As presented in Figure 5c,d the bundles of cellulose are well divided into individual microsized fibers via consecutive elimination of lignin (binding material) and thus breaking the bond between them by bleaching treatment. These individual fibers exhibit an unaligned and random structure. They are entangled and superimposed, with uneven size. The length of the observed fibers (a few hundred  $\mu\text{m}$ ) always remains much greater than their width (from 25 to 30  $\mu\text{m}$ ). The reactivity and the good mechanical adhesion with other polymeric materials could be favored by the presence of different sizes of cellulose fibrils [64].

#### 4. Conclusions

In the present work, cellulose fibers were successfully extracted from a natural source, *Ziziphus jujuba*, using ultrasounds as an alternative energy source for alkali and bleaching treatments. Increasing cellulose while decreasing the hemicellulose and lignin content in the fibers validated the efficiency of the investigated chemical treatment. This was confirmed by the FTIR, where the disappearance of the characteristic bands of lignin and hemicellulose (characteristic band located at  $1734\text{ cm}^{-1}$  attributed to the C=O stretching vibration of p-coumaric acids of lignin and/or hemicellulose). The characteristic bands were located at  $1508\text{ cm}^{-1}$  (C=C of aromatic rings of lignin) and at  $1236\text{ cm}^{-1}$  (C-O groups of methoxy of lignin). In addition, the purified cellulose fibers preserved the structure of cellulose I with nanometric size (10.12 nm), higher crystallinity (57.50%) and good thermal stability ( $220\text{ }^{\circ}\text{C}$ ). Based on the morphological analysis, it can be concluded that the *Ziziphus jujuba* fibers were well divided into individual microsized fibers with random structures and have the advantage of retaining a crystalline (useful for strength) and amorphous structure (interesting for chemical reactivity). The present results reveal the great potential of such cellulose-based fibers as fillers for the development of a new generation of sustainable biocomposites with biodegradable character. Cellulose fibers from *Ziziphus jujuba* could be also modified through grafting phosphorous compounds, and serve for the development of flame-retardant biobased composites.

**Author Contributions:** Conceptualization, A.A. and H.S.; methodology, A.A. and H.S.; software, A.A.; validation, A.A. and H.S.; formal analysis, F.L. and A.A.; investigation, A.A.; resources, A.A.; data curation, A.A.; writing—original draft preparation, A.A. and H.S.; writing—review and editing, F.L., A.T. and P.D.; visualization, F.L. and A.A.; supervision, H.S.; project administration, H.S.; funding acquisition, H.S. All authors have read and agreed to the published version of the manuscript.

**Funding:** This research received no external funding.

**Institutional Review Board Statement:** Not applicable.

**Informed Consent Statement:** Informed consent was obtained from all subjects involved in the study.

**Data Availability Statement:** Not applicable.

**Acknowledgments:** The authors gratefully acknowledge DGRSDT (la Direction Générale de la Recherche Scientifique et du Développement Technologique, Algérie) for its support in this work.

**Conflicts of Interest:** The authors declare no conflict of interest.

## References

1. Siva, R.; Valarmathi, T.N.; Palanikumar, K.; Samrot, A.V. Study on a novel natural cellulosic fiber from *Kigelia africana* fruit: Characterization and analysis. *Carbohydr. Polym.* **2020**, *244*, 116494. [[CrossRef](#)] [[PubMed](#)]
2. Ramesh, M.; Palanikumar, K.; Reddy, H.K. Plant fibre based bio-composites: Sustainable and renewable green materials. *Renew. Sustain. Energy Rev.* **2017**, *79*, 558–584. [[CrossRef](#)]
3. Ding, L.; Han, X.; Cao, L.; Chen, Y.; Ling, Z.; Han, J.; He, S.; Jiang, S. Characterization of natural fiber from manau rattan (*Calamus manan*) as a potential reinforcement for polymer-based composites. *J. Bioresour. Bioprod.* **2022**, *7*, 190–200. [[CrossRef](#)]
4. Satha, H.; Kouadri, I.; Benachour, D. Thermal, Structural and Morphological Studies of Cellulose and Cellulose Nanofibers Extracted from Bitter Watermelon of the Cucurbitaceae Family. *J. Polym. Environ.* **2020**, *28*, 1914–1920. [[CrossRef](#)]
5. Du, H.; Liu, W.; Zhang, M.; Si, C.; Zhang, X.; Li, B. Cellulose nanocrystals and cellulose nanofibrils based hydrogels for biomedical applications. *Carbohydr. Polym.* **2019**, *209*, 130–144. [[CrossRef](#)] [[PubMed](#)]
6. Asif, M.; Ahmed, D.; Ahmad, N.; Qama, M.T.; Alruwaili, N.K.; Bukhari, S.N.A. Extraction and characterization of microcrystalline cellulose from *Lagenaria Siceraria* fruit predicles. *Polymers* **2022**, *14*, 1867. [[CrossRef](#)] [[PubMed](#)]
7. Khandanlou, R.; Ngoh, G.C.; Chong, W.T. Feasibility Study and Structural Analysis of Cellulose Isolated from Rice Husk: Microwave Irradiation, Optimization, and Treatment Process Scheme. *BioResources* **2016**, *11*, 5751–5766. [[CrossRef](#)]
8. Melikoğlu, A.Y.; Bilek, S.E.; Cesur, S. Optimum alkaline treatment parameters for the extraction of cellulose and production of cellulose nanocrystals from apple pomace. *Carbohydr. Polym.* **2019**, *215*, 330–337. [[CrossRef](#)]
9. Sai Prasanna, N.; Mitra, J. Isolation and characterization of cellulose nanocrystals from *Cucumis sativus* peels. *Carbohydr. Polym.* **2020**, *247*, 116706. [[CrossRef](#)]
10. Wang, J.; Han, X.; Zhang, C.; Liu, K.; Duan, G. Source of Nanocellulose and Its Application in Nanocomposite Packaging Material: A Review. *Nanomaterials* **2022**, *12*, 3158. [[CrossRef](#)]
11. Han, X.; Ding, L.; Tian, Z.; Song, Y.; Xiong, R.; Zhang, C.; Han, J.; Jiang, S. Potential new material for optical fiber: Preparation and characterization of transparent fiber based on natural cellulosic fiber and epoxy. *Int. J. Biol. Macromol.* **2022**, *224*, 1236–1243. [[CrossRef](#)] [[PubMed](#)]
12. Reshmy, R.; Philip, E.; Paul, S.A.; Madhavan, A.; Sindhu, R.; Binod, P.; Pandey, A.; Sirohi, R. Nanocellulose-based products for sustainable applications—recent trends and possibilities. *Rev. Environ. Sci. Biotechnol.* **2020**, *19*, 779–806. [[CrossRef](#)]
13. Adeli, M.; Samavati, V. Studies on the steady shear flow behavior and chemical properties of water-soluble polysaccharide from *Ziziphus lotus* fruit. *Int. J. Biol. Macromol.* **2015**, *72*, 580–587. [[CrossRef](#)] [[PubMed](#)]
14. Basyony, M.M.; Elsheikh, H.A.; Abdel Salam, H.S.; Mohamed, K.I.; Zedan, A.H. Utilization of *Ziziphus spina-christi* leaves as a natural growth promoter in rabbit's rations. *EJRS* **2017**, *27*, 427–446. [[CrossRef](#)]
15. Hassainia, A.; Satha, H.; Boufi, S. Chitin from *Agaricus bisporus*: Extraction and characterization. *Int. J. Biol. Macromol.* **2018**, *117*, 1334–1342. [[CrossRef](#)]
16. Hassainia, A.; Satha, H.; Boufi, S. Two Routes to Produce Chitosan from *Agaricus bisporus*. *J. Renew. Mater.* **2020**, *8*, 101–111. [[CrossRef](#)]
17. Kouadri, I.; Satha, H. Extraction and characterization of cellulose and cellulose nanofibers from *Citrullus colocynthis* seeds. *Ind Crops Prod.* **2018**, *124*, 787–796. [[CrossRef](#)]
18. Bouregghda, Y.; Satha, H.; Bendebane, F. Chitin–Glucan Complex from *Pleurotus ostreatus* Mushroom: Physicochemical Characterization and Comparison of Extraction Methods. *J. Waste Biomass Valorization* **2021**, *12*, 6139–6153. [[CrossRef](#)]
19. Sluiter, A. *Determination of Structural Carbohydrates and Lignin in Biomass: Laboratory Analytical Procedure (LAP)*; National Renewable Energy Laboratory: Golden, CO, USA, 2011.
20. Segal, L.; Creely, L.; Martin, A.E.; Conrad, M. An empirical method for estimating the degree of crystallinity of native cellulose using the X-ray diffractometer. *Text. Res. J.* **1958**, *29*, 786–794. [[CrossRef](#)]
21. Makhoulouf, A.; Layachi, A.; Kouadri, I.; Belaadi, A.; Satha, H. Structural study and thermal behavior of composites: Polyamide 66/glass fibers: The reinforcement ration effect on the kinetics of crystallization. *J. Compos. Mater.* **2020**, *54*, 1467–1481. [[CrossRef](#)]
22. Maepa, C.E.; Jayaramudu, J.; Okonkwo, J.O.; Ray, S.S.; Sadiku, E.R.; Ramontja, J. Extraction and characterization of natural cellulose fibers from maize tassel. *Int. J. Polym. Anal. Charact.* **2015**, *20*, 99–109. [[CrossRef](#)]
23. Zhao, G.; Du, J.; Chen, W.; Pan, M.; Chen, D. Preparation and thermostability of cellulose nanocrystals and nanofibrils from two sources of biomass: Rice straw and poplar wood. *Cellulose* **2019**, *26*, 8625–8643. [[CrossRef](#)]
24. Fareez, I.M.; Ibrahim, N.A.; Yaacob, W.; Razali, N.A.M.; Jasni, A.H.; Aziz, F.A. Characteristics of cellulose extracted from *Josapine* pineapple leaf fibre after alkali treatment followed by extensive bleaching. *Cellulose* **2018**, *25*, 4407–4421. [[CrossRef](#)]



25. Yue, Y.; Han, J.; Han, G.; Aita, G.M.; Wu, Q. Cellulose fibers isolated from energycane bagasse using alkaline and sodium chlorite treatments: Structural, chemical and thermal properties. *Ind. Crops Prod.* **2015**, *76*, 355–363. [[CrossRef](#)]
26. Sarikanat, M.; Seki, Y.; Sever, K.; Durmuskahya, C. Determination of properties of *Althaea officinalis* L. (Marshmallow) fibers as a potential plant fiber in polymeric composite materials. *Compos. B. Eng.* **2014**, *57*, 180–186. [[CrossRef](#)]
27. Senthamaraikannan, P.; Saravanakumar, S.S.; Arthanarieswaran, V.P.; Sugumaran, P. Physicochemical properties of new cellulosic fibers from bark of *Acacia planifrons*. *Int. J. Polym. Anal. Char.* **2016**, *21*, 207–213. [[CrossRef](#)]
28. Tanpichai, S.; Witayakran, S. All-cellulose composite laminates prepared from pineapple leaf fibers treated with steam explosion and alkaline treatment. *J. Reinf. Plast. Compos.* **2017**, *36*, 1146–1155. [[CrossRef](#)]
29. Vijay, R.; Manoharan, S.; Arjun, S.; Vinod, A.; Singaravelu, D.L. Characterization of silane-treated and untreated natural fibers from stem of *Leucasaspera*. *J. Nat. Fibers* **2020**, *18*, 1–17.
30. Vinod, A.; Vijay, R.; Lenin Singaravelu, D.; Sanjay, M.R.; Siengchin, S.; Moure, M.M. Characterization of untreated and alkali treated natural fibers extracted from the stem of *Catharanthusroseus*. *Mater. Res. Express.* **2019**, *6*, 085406. [[CrossRef](#)]
31. Khan, A.; Vijay, R.; Singaravelu, D.L.; Sanjay, M.R.; Siengchin, S.; Verpoort, F.; Alamry, K.A.; Asiri, A.M. Extraction and characterization of natural fiber from eleusine indica grass as reinforcement of sustainable fiber-reinforced polymer composites. *J. Nat. Fibers* **2019**, *18*, 1–9. [[CrossRef](#)]
32. Balaji, A.N.; Nagarajan, K.J. Characterization of alkali treated and untreated new cellulosic fiber from Saharan Aloe vera cactus leaves. *Carbohydr. Polym.* **2017**, *174*, 200–208.
33. Reddy, K.O.; Ashok, B.; Reddy, K.R.N.; Feng, Y.E.; Zhang, J.; Rajulu, A.V. Extraction and characterization of novel lignocellulosic fibers from *Thespesia lampas* plant. *Int. J. Polym. Anal. Char.* **2014**, *19*, 48–61. [[CrossRef](#)]
34. Suryanto, H.; Marsyahyo, E.; Irawan, Y.S.; Soenoko, R. Morphology, structure, and mechanical properties of natural cellulose fiber from mending grass (*Fimbristylisglobulosa*). *J. Nat. Fibers* **2014**, *11*, 333–351. [[CrossRef](#)]
35. Fiore, V.; Scalici, T.; Valenza, A. Characterization of a new natural fiber from *Arundodonax* L. as potential reinforcement of polymer composites. *Carbohydr. Polym.* **2014**, *106*, 77–83. [[CrossRef](#)]
36. Raja, K.; Prabu, B.; Ganeshan, P.; Chandra Sekar, V.S.; NagarajaGanesh, B. Characterization studies of natural cellulosic fibers extracted from shwetark stem. *J. Nat. Fibers* **2020**, *18*, 1–14. [[CrossRef](#)]
37. Ganapathy, T.; Sathiskumar, R.; Senthamaraikannan, P.; Saravanakumar, S.S.; Khan, A. Characterization of raw and alkali treated new natural cellulosic fibres extracted from the aerial roots of banyan tree. *Int. J. Biol. Macromol.* **2019**, *138*, 573–581. [[CrossRef](#)]
38. Manimaran, P.; Saravanan, S.P.; Sanjay, M.R.; Siengchin, S.; Jawaid, M.; Khan, A. Characterization of new cellulosic fiber: *Dracaena reflexa* as a reinforcement for polymer composite structures. *J. Mater. Res. Technol.* **2019**, *8*, 1952–1963. [[CrossRef](#)]
39. Moshi, A.A.M.; Ravindran, D.; Bharathi, S.R.S.; Indran, S.; Saravanakumar, S.S.; Liu, Y. Characterization of a new cellulosic natural fiber extracted from the root of *Ficus religiosa* tree. *Int. J. Biol. Macromol.* **2020**, *142*, 212–221. [[CrossRef](#)]
40. Kommula, V.P.; Reddy, K.O.; Shukla, M.; Marwala, T.; Reddy, E.V.S.; Rajulu, A.V. Extraction, modification, and characterization of natural ligno-cellulosic fiber strands from napier grass. *Int. J. Polym. Anal. Char.* **2016**, *21*, 18–28. [[CrossRef](#)]
41. Palacios Hinestroza, H.; Hernandez Diaz, J.A.; Esquivel Alfaro, M.; Toriz, G.; Rojas, O.J.; Sulbaran-Rangel, B.C. Isolation and Characterization of Nanofibrillar Cellulose from *Agave tequilana* Weber Bagasse. *Adv. Mater. Sci. Eng.* **2019**, *2019*, 1342547. [[CrossRef](#)]
42. Kozłowski, R.; Władyska-Przybylak, M. Flammability and fire resistance of composites reinforced by natural fibers. *Polym. Adv. Technol.* **2008**, *19*, 446–453. [[CrossRef](#)]
43. Porras, A.; Maranon, A.; Ashcroft, I.A. Characterization of a novel natural cellulose fabric from *Manicariasaccifera* palm as possible reinforcement of composite materials. *Compos. B. Eng.* **2015**, *74*, 66–73. [[CrossRef](#)]
44. Jothibasu, S.; Mohanamurugan, S.; Vinod, A. Influence of chemical treatments on the mechanical characteristics of areca sheath flax fibres based epoxy composites. *J. Chem.* **2018**, *11*, 1255–1262.
45. Kouadri, I.; Layachi, A.; Makhlouf, A.; Satha, H. Optimization of extraction process and characterization of water-soluble polysaccharide (Galactomannan) from Algerian biomass; *Citrullus colocynthis* seeds. *Int. J. Polym. Anal. Charact.* **2018**, *23*, 362–375. [[CrossRef](#)]
46. Khenblouche, A.; Bechki, D.; Gouamid, M.; Charradi, K.; Segni, L.; Hadjadj, M.; Boughali, S. Extraction and characterization of cellulose microfibrils from *Retamaraetam* stems. *Polímeros.* **2019**, *29*, 1–8. [[CrossRef](#)]
47. Amior, A.; Kouadri, I.; Makhlouf, A.; Satha, H. Extraction process of Galactomannan from Algerian biomass; optimization and physico-chemical analysis. In Proceedings of the Fifth International Conference on Biobased Materials and Composites: ICBMC, Monastir, Tunisia, 17–20 March 2019.
48. Mohamed, N.A.N.; Jai, J. Response surface methodology for optimization of cellulose extraction from banana stem using NaOH-EDTA for pulp and paper making. *Heliyon* **2022**, *8*, e09114. [[CrossRef](#)]
49. Tanpichai, S.; Mekcham, S.; Kongwittaya, C.; Kiwijaroun, W.; Thongdonsun, K.; Thongdeelerd, C.; Boonmahitthisud, A. Extraction of Nanofibrillated Cellulose from Water Hyacinth Using a High Speed Homogenizer. *J. Nat. Fibers* **2021**, *19*, 5676–5696. [[CrossRef](#)]
50. Rohadi, T.N.T.; Ridzuan, M.J.M.; Majid, M.S.A.; Khasri, A.; Sulaiman, M.H.J. *Mater. Res. Technol.* **2020**, *9*, 15057–15071.
51. Johar, N.; Ahmad, I.; Dufresne, A. Extraction, preparation and characterization of cellulose fibres and nanocrystals from rice husk. *Ind. Crops Prod.* **2012**, *37*, 93–99. [[CrossRef](#)]
52. Saravanakumar, S.S.; Kumaravel, A.; Nagarajan, T.; Moorthy, I.G. Investigation of physico-chemical properties of alkali-treated *Prosopis juliflora* fibers. *Int. J. Polym. Anal. Charact.* **2014**, *19*, 309–317. [[CrossRef](#)]



53. Senthamaraikannan, P.; Kathiresan, M. Characterization of raw and alkali treated new natural cellulosic fiber from *Coccinia grandis* L. *Carbohydr. Polym.* **2018**, *186*, 332–343. [[CrossRef](#)] [[PubMed](#)]
54. Yue, Y.; Han, J.; Han, G.; Zhang, Q.; French, A.D.; Wu, Q. Characterization of cellulose I/II hybrid fibers isolated from energycane bagasse during the delignification process: Morphology, crystallinity and percentage estimation. *Carbohydr. Polym.* **2015**, *133*, 438–447. [[CrossRef](#)]
55. Ciftci, D.; Flores, R.A.; Saldaña, M.D.A. Cellulose fiber isolation and characterization from sweet blue lupin hull and canola straw. *J. Environ. Polym. Degrad.* **2018**, *26*, 2773–2781. [[CrossRef](#)]
56. Bharathiraja, B.; Sudharsanaa, T.; Bharghavi, A.; Sowmeya, G.S.; Balaram, G. Insights on lignocellulosic pretreatments for biofuel production—SEM and reduction of lignin analysis. *Int. J. ChemTech Res.* **2014**, *6*, 4334–4444.
57. Cullity, B.D. *Elements of X-ray Diffraction*, 2nd ed.; Addison–Wesley: New York, NY, USA, 1978.
58. NagarajaGanesh, B.; Ganeshan, P.; Ramshankar, P.; Raja, K. Assessment of natural cellulose fibers derived from *Senna auriculata* for making light weight industrial biocomposites. *Ind. Crops Prod.* **2019**, *139*, 111546. [[CrossRef](#)]
59. Tanpichai, S.; Witayakran, S.; Srimarut, Y.; Woraprayote, W.; Malila, Y. Porosity, density and mechanical properties of the paper of steam exploded bamboo microfibrils controlled by nanofibrillated cellulose. *J. Mater. Res. Technol.* **2019**, *8*, 3612–3622. [[CrossRef](#)]
60. Khawas, P.; Deka, S.C. Isolation and characterization of cellulose nanofibers from culinary banana peel using high-intensity ultrasonication combined with chemical treatment. *Carbohydr. Polym.* **2016**, *137*, 608–616. [[CrossRef](#)]
61. Brebu, M.; Vasile, C. Thermal degradation of lignin—A review. *Cellul. Chem. Technol.* **2010**, *44*, 353–363.
62. Mouhoubi, S.; Bourahli, M.E.H.; Osmani, H.; Abdeslam, S. Effect of alkali treatment on alfa fibers behavior. *J. Nat. Fibers* **2017**, *14*, 239–249. [[CrossRef](#)]
63. Yan, L.; Chouw, N.; Yuan, X.J. Experimental Investigation and Analysis of Mercerized and Citric Acid Surface Treated Bamboo Fiber Reinforced Composite. *Reinf. Plast. Compos.* **2012**, *31*, 425–437. [[CrossRef](#)]
64. Kargarzadeh, H.; Ahmad, I.; Abdullah, I.; Dufresne, A.; Zainudin, S.Y.; Sheltami, R.M. Effects of hydrolysis conditions on the morphology, crystallinity, and thermal stability of cellulose nanocrystals extracted from kenaf bast fibers. *Cellulose* **2012**, *19*, 855–866. [[CrossRef](#)]
65. Ouarhim, W.; Essabir, H.; Bensalah, M.; Zari, N.; Bouhfid, R. Structural laminated hybrid composites based on raffia and glass fibers: Effect of alkali treatment, mechanical and thermal properties. *Compos. B* **2018**, *154*, 128–137. [[CrossRef](#)]

**Disclaimer/Publisher’s Note:** The statements, opinions and data contained in all publications are solely those of the individual author(s) and contributor(s) and not of MDPI and/or the editor(s). MDPI and/or the editor(s) disclaim responsibility for any injury to people or property resulting from any ideas, methods, instructions or products referred to in the content.